NJC

Accepted Manuscript

This is an *Accepted Manuscript*, which has been through the Royal Society of Chemistry peer review process and has been accepted for publication.

Accepted Manuscripts are published online shortly after acceptance, before technical editing, formatting and proof reading. Using this free service, authors can make their results available to the community, in citable form, before we publish the edited article. We will replace this *Accepted Manuscript* with the edited and formatted *Advance Article* as soon as it is available.

You can find more information about *Accepted Manuscripts* in the Information for Authors.

Please note that technical editing may introduce minor changes to the text and/or graphics, which may alter content. The journal's standard Terms & Conditions and the Ethical guidelines still apply. In no event shall the Royal Society of Chemistry be held responsible for any errors or omissions in this *Accepted Manuscript* or any consequences arising from the use of any information it contains.

ROYAL SOCIETY OF CHEMISTRY

www.rsc.org/njc

New journal of chemistry

RSCPublishing

ARTICLE

Theoretical investigation on a series of novel *S,S*-dioxide diarylethenes with abnormal photochromic properties and design of new dyads

Zhi-Xiang Zhang, Fu-Quan Bai*,[b] Li Li, Hong-Xing Zhang*,[a]

Density functional theory (DFT) calculations are utilized to analyze a novel *S,S*-dioxide diarylethene of which, contrary to general ones, ring-closing happens under visible light (436 nm) and ring-opening arises in ultraviolet light (365 nm). The asymmetrical structure and the oxidized S atoms alter the continuity and switch way of conjugation system between two isomers. The role and position of substituent affect the intramolecular electron transfer in reaction and result in changes in conversion ratio and quantum yield. Based on the diarylethene, we designed new dyads in which ring–closing and -opening of the two diarylethene parts in one molecule proceed simultaneously under single wavelength. The photocyclization on one part of the molecule does not limit but facilitate the photocycloreversion on the other part.

Introduction

Photochromic materials, due to their interesting optical properties, have attracted a lot of attention since they were synthesized and used into practical application. Among various of photochromic materials, the treated representative one is diarylethene [1]. A reversible photocyclization and photocycloreversion for diarylethene can proceed under different wavelength irradiation, which makes an exchange between open-ring or closed-ring isomers. The isomers show the same favourable thermal stability but different behaviours in absorption, solvent colour, electric conduction, fluorescence and so on. These special behaviours impel diarylethene to be widely applied in optical instruments, such as information transfer, data storage, molecular switch, fluorescence label, *etc*. [2, 3].

A general diarylethene consists of two parts, which is that two identical aromatic rings are connected by a C=C double bond in the same way to generate a six-member open-ring structure. The open-ring form can be induced to undergo photocyclization to become closed-ring form by ultraviolet light irradiation and reverse back through photocycloreversion using visible light irradiation. However, Masahiro Irie and co-workers [4] synthesized a series of novel diarylethenes on the basis of **1** which has two different aromatic rings (Scheme 1 where 'a' refers to the open-ring form and 'b' refers to the closed-ring form, and it is same in the following depiction. Not involved in experiment, **1** is only mentioned to help explaining our work). This difference leads to the significant change of their optical properties as compared with common ones. For instance, the photocyclization of new diarylethene could proceed upon irradiation with visible wavelength (450 nm) and photocycloreversion became feasible under ultraviolet wavelength (365 nm). When the molecule was connected with other groups in different positions (**2**, **3** and **4**, **5** in Scheme 1), the properties including fluorescence effect, conversion ratio, and quantum yield also changed a lot.

In experiment, there are many synthesized compounds containing diarylethenes and different fluorescent groups [5-8]. These compounds have better properties in optical performance. They show fluorescence response in open-ring isomers but lose it in the closed-ring ones. Two kinds of mechanisms are employed to explain the phenomenon, intramolecular energy transfer [7] and intramolecular electron transfer (IET) mechanisms [8]. These compounds are treated as a new kind of nondestructive readout materials. Though they perform properly, there are still some other problems unsatisfied, such as low fluorescence quantum yield, low quenching and reaction efficiency. Masahiro Irie and co-workers also examined their novel diarylethene on fluorescence application [9]. They developed **4** and **5** (Scheme 1) which were composed of the novel diarylethene (**DE**) and a fluorescent perylenebisimide (**PBI**). Further testing found that **4** avoided the ring-open side-reaction and showed expected fluorescence performance. When **DE** was in open-ring form, **PBI** showed absorption at 524 nm and emitted fluorescence at 537 nm in 1, 4-dioxane solution. If **DE** was in closed-ring form and the solvent polarity was increased, the fluorescence intensity weakens dramatically. It was more obvious within more polar solvent. However, the introduction of **PBI** brought in another unexpected side reaction. The open-ring **DE** proceeded with photocyclization through a triplet state way. In order to solve this problem, **4** was modified to red shift the absorption spectra of **PBI**, trying to make its first singlet excited state S_1 lower than the first triplet excited state of **DE**. At last, an excellent compound corresponding with all purposes andrequirements wherever in solution or at single-molecule level was synthesized successfully [10].

a,b *Dr. Z.X. Zhang, Prof. F. Q. Bai, Dr. L. Li, Prof. H. X. Zhang*
State Key Laboratory of Theoretical and Computational Chemistry, Institute of Theoretical Chemistry
Jilin University
Changchun 130023, (PRC)

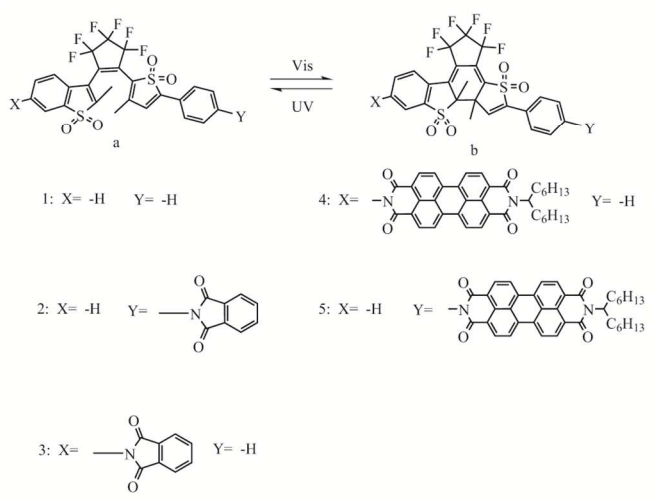

Scheme 1. Structures of the series of novel diarylethenes with different substituent.

It is all the aforementioned that attract our interest to these novel diarylethenes. So we employed density functional theory (DFT) as method to have research on their geometry structures, absorption spectra, energies, molecular orbitals, and electron transfer trend, trying to give theoretical explanation for the experimental phenomenon. It would be better if we could make some suggestions on synthesizing and the capability improvement.

Computational methods

Density functional theory (DFT) method [11-13] was used in our calculation as it could consider the electronic correlation well and be applied to most of organic molecules with sufficient accuracy. The results depending on this method scheme were worth affirmative. [14, 15] At first full geometry optimizations of all molecules was performed using B3LYP(Becke's three parameter functional and Lee-Yang-Parr functional) functional and standard 6-31G (d) basis set was used to describe the atoms. Frequency calculations were used to ensure that the ground-state geometry corresponds to the minimum point of potential energy surface. Natural bond orbital (NBO) analysis was utilized to study the electronic charges of every atom. Time-dependent density functional theory (TDDFT) [15-17] was adopted to calculate the vertical excited energy and absorption spectra of the optimized molecules. The solvent effect was included by mean of polarizable continuum model (PCM) [18] which can offer non-equilibrium linear approximation in TDDFT calculation. The experimental spectra are carried out in 1, 4-dioxane, a nonpolar and aprotic solvent, so PCM, which neglects solute-solvent interaction, can be applied straightforwardly. The hypochromatic or hyperchromatic shift of absorption spectra upon photochromic reactions are attributed to the exchange of conjugation system and geometries in molecule. In order to select a suitable functional to describe the exchange and correspond to experimental data, consistent calculations including structures, absorption spectra, and transition energies should be computed with the selected approach. For instance, Mennucci[19] and co-workers performed simulations of the 0-0 optical energies of 40 fluorescent molecules. Furche[20] and co-workers utilized Adiabatic Excitation Energy (AEE) to assess sexcited state methods. They have proved that one functional cannot be suitable to every molecule. In our calculation, we evaluated some functionals, such as CAM-B3LYP [21], PBE0 [22], BMK [23], BHandH [24], and B3P86 [25]. These functionals have been widely used on various organic molecules in TDDFT calculations [15, 16, 26, 27] and the results which include the description of excitation, the absorption spectra, and excited energy are in good agreement with experiment. The data of each isomer of **1**-**5** is listed in Table 1. We have compared the results of every functional and found that, despite the difference on orbital energies, the similarities on the distributions of frontier molecular orbitals and Electron transition configurations are rather high. It is found that to the molecules without fluorescence groups (**2**, **3**), CAM-B3LYP was thought to be satisfactory, while PBE0 did well in simulating on the molecules owning fluorescence groups (**4**, **5**). It is reasonable because PBE0 includes a constant fraction of exact exchange. In CAM-B3LYP a growing fraction of Hartree–Fock-like exchange is used when the inter-electronic distance increases. Considering the magnitude of error, a compromise result belonging to PBE0 is chosen in our discussion. The comparison between experimental and calculated spectra is shown in Figure 1 in which **4** is used as an example. Gaussian09 program package [28] was used in all the calculations.

Table 1. The results of absorption maxima (nm) of every isomer in 1, 4-dioxane solution, obtained by TD-DFT calculations with different functional under 6-31G(d) basis set. The experimental data is shown for comparison.

		CAM-B3LYP	PBE0	BMK	BHandH	B3P86	B3LYP	Exp.[a]
1a		361	394	370	359	406	406	-
1b		340	362	345	337	370	409	-
2a		377	419	390	376	433	434	379
2b		341	363	341	338	371	371	352
3a		365	402	375	364	416	416	356
3b		357	389	364	354	397	410	374
4a	**PBI**[b]	474	520	486	473	533	535	524
	DE[c]	364	399	374	362	411	411	369
4b	**PBI**[b]	476	522	488	475	535	537	525
	DE[c]	348	374	354	344	382	384	358
5a	**PBI**[b]	474	520	486	473	533	534	522
	DE[c]	368	404	378	366	417	417	368
5b	**PBI**[b]	473	518	485	472	532	533	522
	DE[c]	341	362	346	338	411	370	352

[a] The data comes from reference 4 and 10. [b] The data corresponds to perylenebisimide (PBI) part. [c] The data corresponding to diarylethene (DE)part.

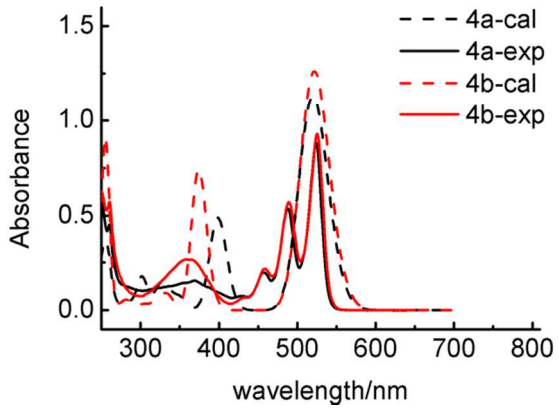

Figure 1. The comparison of absorption spectrums between calculated (cal, dash line) and experimental (exp, solid line) results of **4**. The FWHM used in Gaussian is 0.2eV (1613.11 cm^{-1})

Results and discussions

Analysis of absorption spectra

In this section the hypochromatic shift of absorption spectra is discussed. For discussion convenience, the main atoms of **1** are defined in number and the molecule is divided into three parts, I (red), II (blue), and III (purple) which stand for 2-methyl-1-benzothiophene-1, 1-dioxide-3-yl group, hexafluorocyclopentene, and 3-methyl-5-phenyl -1, 1-dioxide-2-yl group, respectively, as shown in Scheme 2a. Part IV is the substituent in **2** and **3** (Scheme 1). In order to investigate the differences of part I and III [13, 29, 30], we compared the molecular orbital of some symmetrical diarylethenes models with different substituents (**SDE**, Scheme 3) and the results are displayed in Figure 2. For **SDE3S** and **SDE3SO**, whatever S is oxidized or not, the maximum absorption peak has an obvious hyperchromatic shift when cyclization occurs. Because the non-coplanar open-ring isomer converts into a coplanar closed-ring isomer and a large conjugated π bonds surface is formed. The conjugated surface reduces the energy gap between the highest occupied molecular orbital (HOMO) and the lowest unoccupied molecular orbital (LUMO). The same case happens on **SDE2S**. But when S is oxidized in **SDE2SO**, the maximum absorption peak of closed-ring form is hypochromatic shifted. It is inferred that the state of atom S has enormous influence on the absorption spectra shifts. If not oxidized (**SDE2S**), S will participate in making up π bond on thiophene. When one of double bonds on thiophene is dismissed in photocyclization, S still offers p atomic orbitals to sustain a conjugation system through molecule to strength the connection between middle part and side parts (Figure 2- **SDE2Sb**), which is the same as **SDE3S** and **SDE3SO** whose HOMO and LUMO are both distributed continuously on the whole molecule surface (Figure 2- **SDE3Sb**, **SDE3SOb**). If S is oxidized, the conjugation relationship between middle and side parts will be cut off. HOMO has no distribution on middle part. Neither does LUMO on side parts.

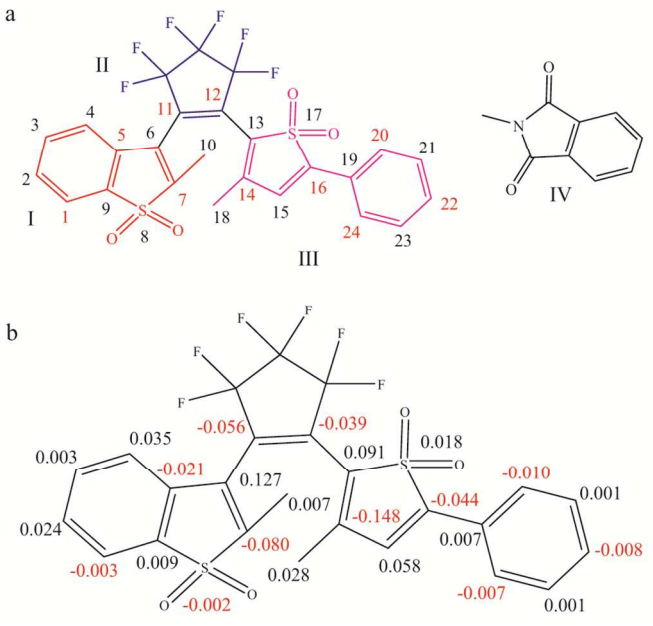

Scheme 2. a) Different parts in novel diarylethene and atoms are ordered in numbers. b) Electrical charge variates of related atoms during photocyclization.

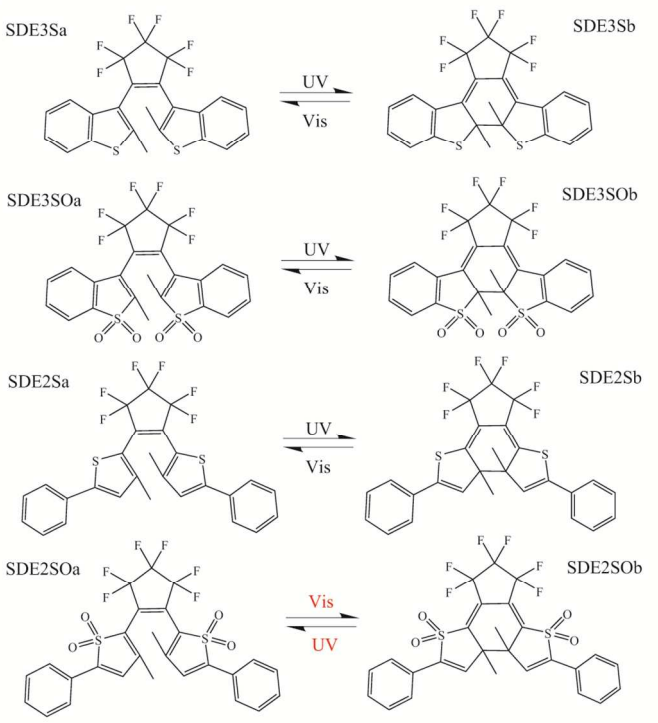

Scheme 3. Structures of **SDE**s with symmetrical substituents.

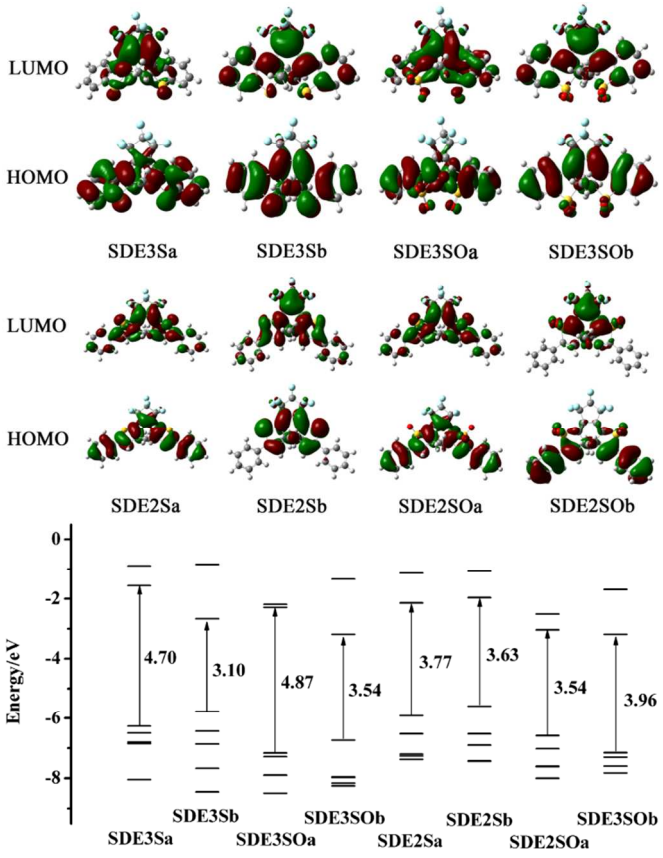

Figure 2. The frontier molecular orbitals and energy level of four **SDE**s.

(Figure 2-**SDE2Sb**).Inefficient orbital overlap of HOMO and LUMO leads the excitation of **SDE2SOb** to take place with intramolecular electron transfer, which is much more difficult than that of **SDE2SOa**. Actually the maximum absorption peak corresponds to HOMO-n→LUMO. Moreover, the photocyclization of **SDE2SO** is a conjugation decreasing process and the energy gap of HOMO and LUMO is increased. According to the two reasons, the absorption spectrum of **SDE2SO** is hypochromatic shifted by photocyclization.[13]

By analogy, a hypochromatic shift similar to **SDE2SO** happens on the new diarylethenes. The results of TD-DFT calculation are listed in Table 2. The main configuration to the maximum absorption peak of open-ring form in **1**, **2**, and **3** is HOMO→LUMO transition. But it turns out to be HOMO-n→LUMO in closed-ring form. Because the different aromatic rings of two sides cannot be treated equally during excitation. More importantly, the oxidation of S in part III is the key to the evident hypochromatic shift in absorption spectrum.

On the other hand, the substituents will affect the whole electronic property of the novel diarylethene, too. For example, in Figure 3-**3a**, **3b**, the distributions of HOMO display an inclination to the position of part IV. Because of this inclination, the order of frontier molecular orbital of **3b** is rearranged and HOMO-1 becomes almost degenerate with HOMO. In our calculation, the absorption peak corresponds to two wavelengths, 389nm and 384nm of which the main transition configurations are composed of HOMO→LUMO and HOMO-1→LUMO (Table 2). Actually the experimental spectra also have proven that the hypochromatic-shift of **3** is not as obvious as **2**. But the reporters stated that they believed the hypochromatic-shift still existed because the absorption of **3a** had larger width in longer wavelength region (>400 nm) compared with **3b** [4].

Analysis of the influence of substituent

The reaction can be explained by the principle of the conservation of molecular orbital symmetry and most of changes happen on the central ring. But the property of substituent and its position in molecule also have significant influences on reaction process. For example, photocyclization conversion ratio difference between **4a** (69%) and **5a** (72%) is small, but becomes very large between **2a** (82%) and **3a** (6%) [4]. The influences can be treated in two ways.

Table 2. Electron transition configurations, excitation energies, and oscillator strengths (f) for main absorption band of isomers. The experimental data is shown for comparison (**1** is not involved in experiment).

	State	Major contrib. [a]	Energy (nm/eV)	*f*	Exp.(nm) [b]
1a	$S_0 \rightarrow S_1$	H→L (98.1%)	394/3.14	0.4826	-
1b	$S_0 \rightarrow S_2$	H–1→L (98.6%)	362/3.43	0.5330	-
2a	$S_0 \rightarrow S_1$	H→L (97.4%)	419/2.95	0.7935	379
2b	$S_0 \rightarrow S_2$	H–1→L (98.8%)	363/3.41	0.5628	352
3a	$S_0 \rightarrow S_1$	H→L (98.0%)	401/3.08	0.4545	356
3b	$S_0 \rightarrow S_1$	H→L (84.7%) H-1→L (13.7%)	389/3.18	0.4566	374
	$S_0 \rightarrow S_2$	H-1→L (84.6%) H→L (14.0%)	384/3.22	0.4820	
4a	$S_0 \rightarrow S_1$	H→L (99.9%)	519/2.38	1.1164	524
	$S_0 \rightarrow S_3$	H-1→L+1 (97.5%)	399/3.11	0.4811	369
4b	$S_0 \rightarrow S_1$	H→L (99.1%)	521/2.38	1.2835	525
	$S_0 \rightarrow S_6$	H-2→L+1 (64.2%)	374/3.31	0.4613	358
5a	$S_0 \rightarrow S_1$	H→L (99.4%)	519/2.39	1.1886	522
	$S_0 \rightarrow S_4$	H-1→L+1 (97.1%)	404/3.07	0.5592	368
5b	$S_0 \rightarrow S_1$	H→L (100.0%)	518/2.39	1.1062	522
	$S_0 \rightarrow S_6$	H-2→L+1 (98.0%)	362/3.42	0.5545	368

[a] 'H' means HOMO and 'L' means LUMO. [b] The data comes from reference 4 and 10.

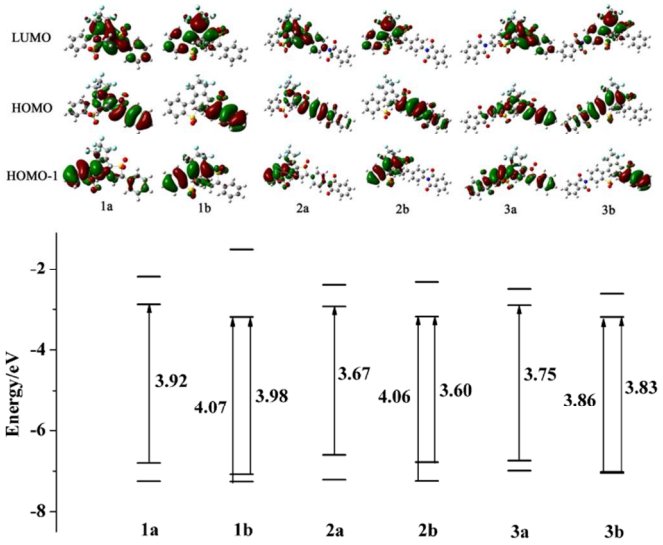

Figure 3. The frontier molecular orbitals and energy level of **1-3**.

The first way is the effect on the distribution of molecular orbital. As mentioned in last section, HOMO and HOMO-1 are almost degenerate. Part IV reduces the difference of excitation energy between **3a** and **3b** in some extent. So irradiation wavelength capable of photocyclization may also induce photocycloreversion, which will reduce the photocyclization conversion. The second way is the contribution to electron transfer. The electrical charge distributions of every part in **1-5** are listed in Table 3. To part I the charge is higher in open-ring form than in closed-ring form, meaning it acts as an electron donor. Similarly, part II and III are electron accepters. It demonstrates that electrons transfer from left to middle and right during photocyclization. This transfer trend is also proved by the behaviour of part IV. It decreases a little (-0.008) in **2** but increases rather much (0.032) in **3**, which implies part IV is a neglectable electron accepter in **2** and an essential electron donor in **3**, respectively. As a non-electron-rich group, part IV suffers to be an electron donor. It may hinder the photocyclization of **3a**. In **2a**, on the contrary, part IV has less effect on the transfer trend and follows it as a supporting group, which should be helpful to photocyclization. So it is believed that the large conversion ratio difference between **2a** and **3a** derives from the different influence of part IV which depends on its position in molecule. In addition, part IV connects with part I by atom C2 of which the charge increases in photocyclization in **3** (Scheme 2b), which may not be beneficial to the electron transfer because of orientation collision. However, the collision does not exist in **2** because the connecting atom is a

Table 3 The charge distributions for different parts of **1-5**. In photocyclization.

	1a	**1b**	**2a**	**2b**	**3a**	**3b**
I	0.009	0.097	0.008	0.107	0.191	0.283
II	-0.061	-0.137	-0.063	-0.137	-0.059	-0.142
III	0.051	0.030	0.245	0.224	0.052	0.027
IV	-	-	-0.190	-0.198	-0.196	-0.164
	4a	**4b**	**5a**	**5b**	**-**	**-**
I	0.223	0.313	0.007	0.107	-	-
II	-0.060	-0.138	-0.061	-0.137	-	-
III	0.054	0.030	0.280	0.255	-	-
PBI	-0.217	-0.205	-0.226	-0.225	-	-

charge-decreasing atom C22. This may explain the rather difference between the conversion ratios of 2a and 3a, too.

Such big difference does not exist between **4a** and **5a** because **PBI** has better flexibility to promote photocyclization. As shown in Figure 4, the introduction of **PBI** makes big molecular orbital distribution change on the basis of **1**. There is no obvious orbital overlap between **PBI** and **1**, which means the excitation of **1** will suffer less perturbation from **PBI**. On the other hand, as a large planar group with high electron densities, **PBI** could be an excellent supportive substituent to the IET process and it can also induce reaction by a triplet way [9] which will be mention in next paragraph.

Compared with conventional ones, the novel molecule has an asymmetrical structure and suffers the difficulty of simultaneous excitation of both part I and III. So its photochromic reactions should be more complex and their quantum yields get lower. A diagram showing the excitation wavelength dependence of photocyclization of **4a** and **5a** in 1, 4-dioxane is displayed in experimental report [4]. In short wavelength (λ<410 nm) region the quantum yield of **4a** increases until it reaches the top (0.013). Then it decreases sharply between 410nm and 460nm, and keeps constant (0.0012) in longer wavelength (λ>460 nm) region. The change of quantum yield suggests the photocyclization proceeds via different pathways upon irradiation with different wavelength light. It must be stated that only **PBI** has absorption in the region between 460 and 530 nm. In other words, when the irradiation wavelength is longer than 460 nm, an IET process from the excited **PBI** to **DE** will take place and induce photocyclization. But an efficient induction should centre on the right side of **DE** (part II and III) which, however, does not connect with **PBI** directly. Because of this structural deficiency against IET process and the indirect excitation, the quantum yield further decreases. On the other hand, the quantum yield of **5a** stays constant (0.015) in the whole wavelength region. It can also be interpreted by the IET process and the direct connection between **PBI** and part III of **DE**. The explanation is supported by the distribution of molecular orbitals (Figure 4). Compared with **4a**, **5a** has successive distribution from HOMO-2 to LUMO+1.

In summary, the substituent mainly influences on the electron transfer process during reaction. The influence is determined by its electronic properties and the connecting position with molecule.

Many researchers have scanned the PES of diarylethene previously and some conclusions have been proposed [11, 14, 31-35]. An excellent work was done by Robb and co-workers [33] who utilized complete active space self-consistent field (CASSCF) method on dithienylethene. They demonstrated that both reactions involve state exchanging through one conical intersection (CI) between S_1 and S_0.

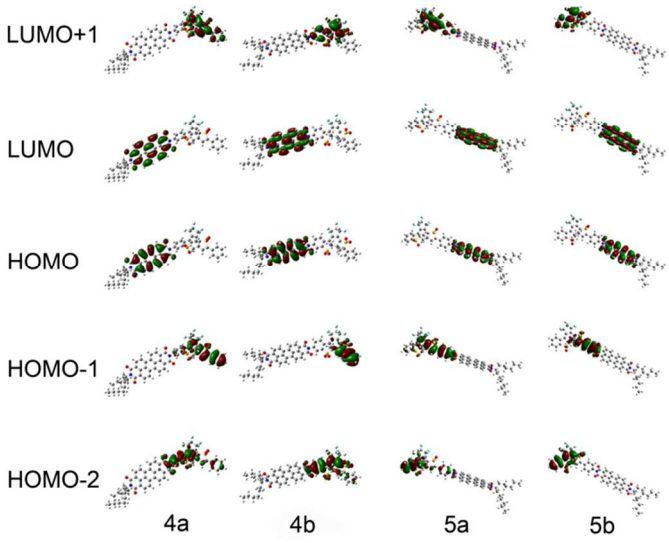

Figure 4. The frontier molecular orbitals of **4** and **5**.

Summarizing from the changes of electrical charge and molecular orbitals, it is inferred that electron transfer proceeds during excitation. The main charge change is concentrated on the central ring (C6, C7, C11-C14). When one atom gets higher in charge, those with it will get lower. For instance, the charges of atoms C in *meta*-positions of benzenes show similar trend, either increase or decrease (Scheme 2b), which agrees with molecular orbital well (Figure 3 LUMO). Plenty of experiments have clarified that the diarylethene photochromic reaction is a picoseconds-scale process [14, 32, 36], which manifests it should be simple. Generally researchers believe the reactions proceed through four states. First the reactant (R) is excited under irradiation. Then it passes through a conical intersection [14, 18] and releases energy to reach the ground state of product (P), in the following way,

$$R\,(S_0) \rightarrow R\,(S_1) \rightarrow R\,(S_1,CI) \xrightarrow{CI} P\,(S_0,CI) \rightarrow P\,(S_0)$$

it is reasonable that R (S_1) changes to P (S_0) directly after passing conical intersection because the molecular orbital shapes on part II show similarities between **2a** LUMO and **2b** HOMO-1, or **2a** HOMO and **2b** LUMO (Figure 3). The ignorance of P (S_1) is the most effective path in which no unnecessary charge redistribution exists. Additionally, according to Table 3, as the electron transfer direction of ring-opening (ring-closing) is from right (left) to left (right), the reactive centre should be located in left (right) parts. It could be evolved that the conical intersection may differ from ring-opening to ring-closing and such two photoreactions may not be totally reciprocal.

New dyads design

Almost all of diarylethene dyads synthesized are composed of two diarylethene parts. They can either be independent to each other or show a restriction relationship in which photocyclization in one part induces an elongation of the reactive CC distance in the other part, making the next photocyclization impossible because of steric and electronic effects [37-41]. Such drawback may be overcome if the novel molecule is utilized in synthesis. Predictably, a visible irradiation on a new dyad which is composed of 1 and another normal diarylethene may induce photocyclization in 1 and photocycloreversion in the other diarylethene simultaneously. Similarly, a reciprocal process can be detected under UV irradiation. The two parts are not independent and do not hinder each other during reactions. Contrarily, they may keep a cooperative relationship which improves the conversion ratio and quantum yield of the dyad, compared with monomers.

Following this idea, some dyads are designed in theoretical level. The two diarylethenes in each dyad are selected according to their inducing conditions [29, 30]. In order to build the ideal relationship mentioned in the last paragraph, they are connected through thienothiophene moiety and the connecting atoms are specifically selected as the ones which show the same electrical charge varying trend in reactions for both sides. After optimization some are abandoned and the rests are displayed in Scheme 4. Their relative energies and geometry data are listed in Table 4. Geometry optimizations reveal that the thienothiophene moiety is slightly bent. The CC distances between the reactive carbon atoms are also reasonable. But there are still some drawbacks. For example, in **D2ab**, some intervals between the hydrogen atoms of the methyl groups are too small (2.00Å)[37], which would imply a weak steric hindrance and do harm to its thermal stability. The electrical charge

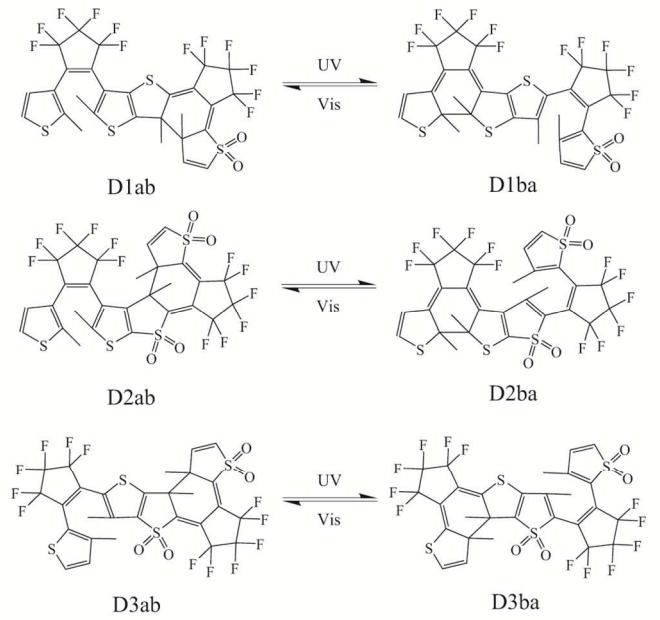

Scheme 4. Structures of designed dyads.

Table 4 Relative energies('Dab' is treated as reference point) and geometry data of every dyad isomer. 'd' repreasents the distance of reactive C atoms. 'D' represents the dihedral angle of the two thiophenes in thienothiophene.

dyad	Relative energy（eV）	d_{open}(Å)	d_{closed}(Å)	D(°)
D1ab	0.00	3.73	1.56	176.0
D1ba	0.04	1.54	3.68	176.6
D2ab	0.00	3.63	1.58	168.0
D2ba	0.19	1.54	3.69	171.7
D3ab	0.00	3.64	1.57	175.5
D3ba	0.94	1.56	3.80	174.4

variates of related atoms during **Dab** → **Dba** is shown in Scheme 5. According to the data, no specific electronic structure modification arises between the two parts. TDDFT is also performed on these dyads. The absorption results are shown in Table 5 and the corresponding molecular orbitals and calculated spectra are listed in Figure 5 and Figure 6, respectively. As shown, the electron transitions of these new dyads are more complicated. Almost all of absorption peaks widths are extended because more than one excitation mode are included. For example, in **D2ab**, the peak ranging from 300nm to 350nm involves four modes ($S_0 \rightarrow S_2$, S_3, S_4, and S_5). These modes correlate with the excitations of both diarylethene parts, meaning that electrons can be promoted towards the efficient orbitals (LUMO and LUOM+1) which present typical topologies for photoreactions[3, 37]. The pity is, proved by the distributions of frontier orbitals (Figure 6), that one single mode only correlates with the excitation of one part, either 'a' or 'b'. It indicates that the relationship between two parts is not as perfectly cooperative as expected. This phenomenon is more obvious in **D1** and **D2** than in **D3**. Moreover, compared with the other two **Dba**s, **D3ba** has no absorption in long wavelength range, which is attributed to its noncontinuous conjugation system, the same as **1**. So **D3** seems to be more successful in aggregation of the two diarylethene parts than the other two dyads and it may show the expected property. But it does not mean **D1** and **D2** are not capable. There are also absorption peaks in the corresponding ranges on their spectra (Figure 6) which

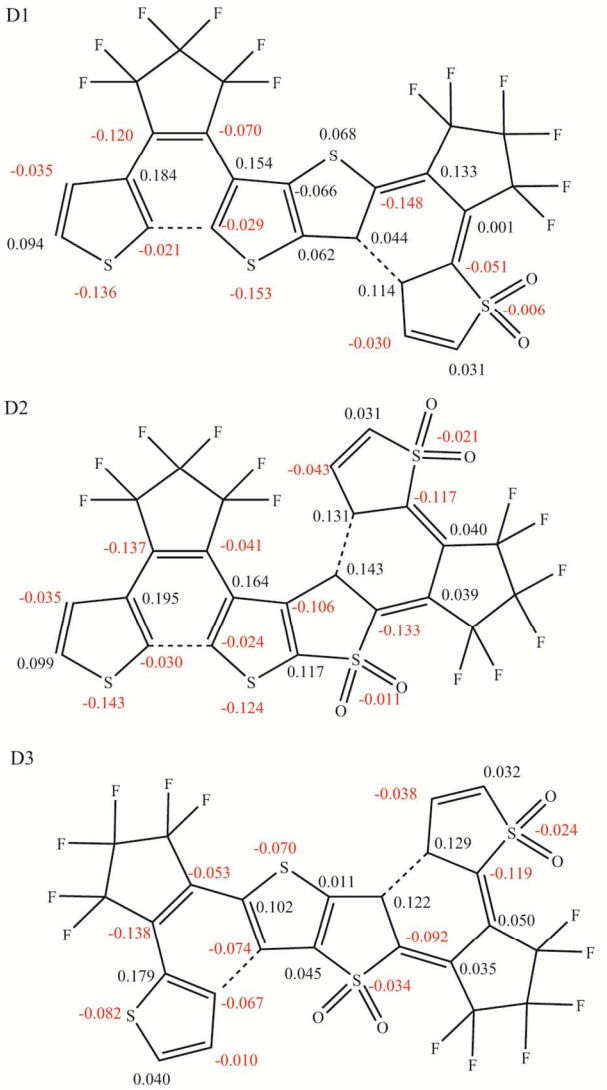

Scheme 5 the electrical charge variates of related atoms during **Dab** → **Dba**. The dash lines represent the bonding or breaking processes in reactions

implies it is possible for the reaction to proceed by carefully selected excitation wavelengths if they can be tested experimentally.

It is understandable that the aggregation of two diarylethenes causes the complexity of electron transition. Though wanted, the complexity may bring side reactions, too. Besides, all of the absorption strengths of the three dyads are low. Admittedly, the dyads are only designed theoretically and their properties are still unknown, but it is worth a shot.

Conclusion

DFT/TD-DFT methods have been applied to probe the ground and excited state of a novel series of *S,S*-dioxide diarylethenes. Specific attentions have been granted to analyze their geometries, distribution of molecular orbitals, electronic transition, and charge transfer. Compared with conventional ones, the two thiophenes in novel diarylethene connect with C=C double bond in different ways and the S atoms are oxidized. Without the involvement of p atomic orbitals from S, closed-ring isomer cannot keep a whole conjugation

system through molecule, which enlarges the energy gap of HOMO and LUMO and makes its absorption spectrum hypochromatic shifted. However, the conjugation system in open-ring isomer is not altered. So singlet wavelength irradiation can only induce one part of molecule and the part differs in two isomers, as show in molecular orbitals. Besides, substituent effect cannot be neglected. It is found that, in different position, the substituent has different influences on the distributions of frontier orbitals and electron transfer trend. The relationship with molecule is determined by its own properties, such as the electron densities and the gain-loss ability, which plays important role in the conversation ratio and quantum yield of photocyclization.

New dyads are designed according to our research above. Compared with normal dyads, new ones have different characteristics in photoreactions. The two diarylethene parts in one dyad can be induced to react by single wavelength irradiation simultaneously. They are not independent and do not suppress each other, but show a cooperation relationship to promote the reactivity of the new dyads. This design is reasonable in theory and needs support from experiment. But it may bring a new idea on the synthesis of diarylethene dyads.

Table 5. Electron transition configurations, excitation energies, and oscillator strengths (f) for main absorption band of three designed dyads. The results are calculated under PBE0/6-31G(d) method.

dyad	State	Major contrib.	Energy(nm/eV)	*f*
D1ab	$S_0 \rightarrow S_1$	H→L (99.0%)	431/2.88	0.1325
	$S_0 \rightarrow S_4$	H-1→L+1 (96.3%)	307/4.04	0.1243
	$S_0 \rightarrow S_5$	H-2→L(79.3%) H-3→L(12.9%)	302/4.11	0.0333
D1ba	$S_0 \rightarrow S_1$	H→L (98.1%)	610/2.03	0.4066
	$S_0 \rightarrow S_4$	H-2→L (88.0%) H-1→L+1 (4.2%)	372/3.33	0.2082
D2ab	$S_0 \rightarrow S_2$	H-2→L (92.0%)	344/3.60	0.0340
	$S_0 \rightarrow S_3$	H-1→L (57.6%) H-3→L (35.1%)	328/3.78	0.0777
	$S_0 \rightarrow S_4$	H→L+1 (87.3%) H-1→L (8.2%)	317/3.92	0.0803
	$S_0 \rightarrow S_5$	H-3→L (55.5%) H-1→L (29.7%) H→L+1 (8.4%)	313/3.96	0.0678
D2ba	$S_0 \rightarrow S_2$	H→L+1 (94.4%)	490/2.53	0.2342
	$S_0 \rightarrow S_3$	H-1→L (95.3%)	414/2.99	0.1232
	$S_0 \rightarrow S_3$	H-2→L+1 (77.2%) H-3→L (7.2%) H-1→L+2 (5.4%)	320/3.88	0.1143
D3ab	$S_0 \rightarrow S_2$	H→L+1 (93.6%) H-2→L (3.6%)	345/3.59	0.3873
	$S_0 \rightarrow S_3$	H-2→L (62.2%) H-1→L (24.3%)	335/3.70	0.0277
	$S_0 \rightarrow S_4$	H-1→L (73.1%) H-2→L (20.6%)	328/3.78	0.0148
D3ba	$S_0 \rightarrow S_2$	H→L+1 (82.1%) H→L (5.8%)	439/2.82	0.0657
	$S_0 \rightarrow S_3$	H→L+2 (86.9%) H-2→L+1 (10.2%)	392/3.16	0.0726
	$S_0 \rightarrow S_4$	H–1→L (92.3%) H–2→L (3.4%)	387/3.20	0.1302

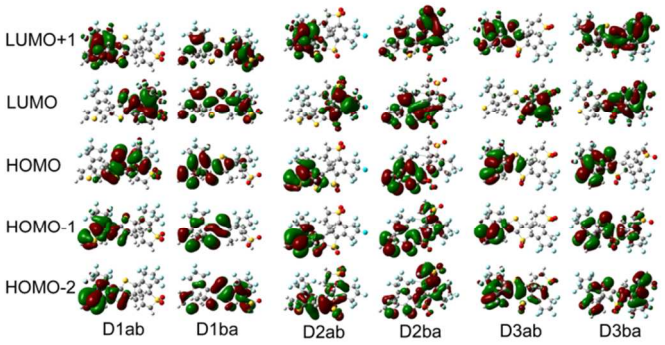

Figure 5. The frontier molecular orbitals of Designed dyads (**D**s).

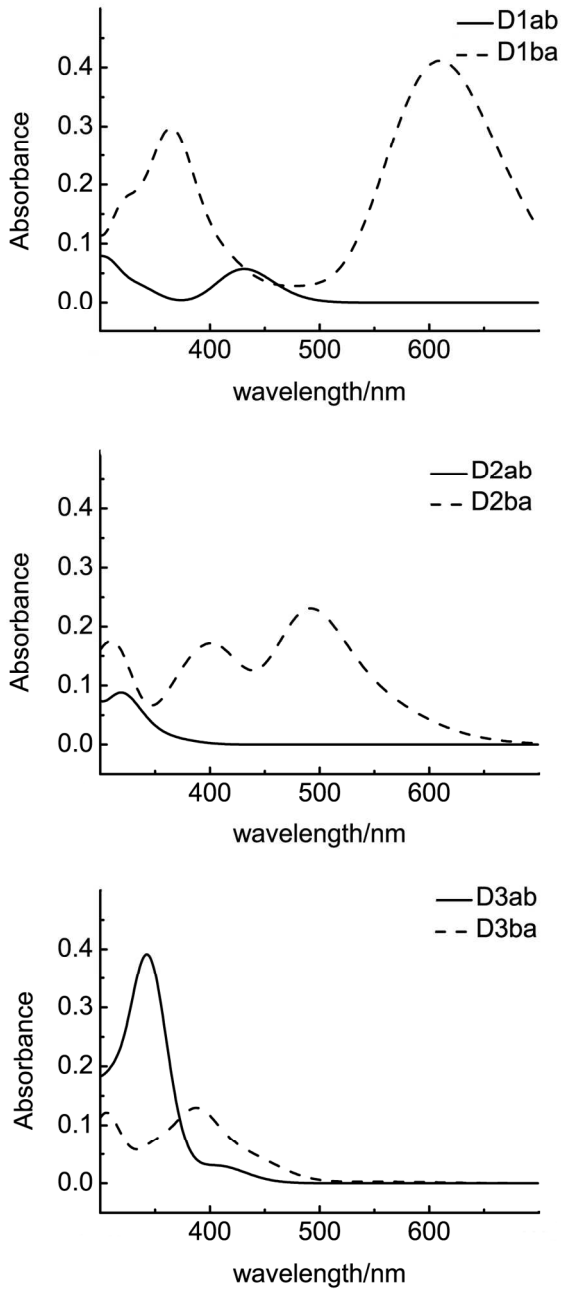

Figure 6. The absorption spectra of **D1**, **D2**, and **D3** by TD-DFT method.

Corresponding author

[a,*] Prof. H-X. Zhang; E-mail: zhanghx@mail.jlu.edu.cn
[b,*] Prof. F-Q. Bai; E-mail: baifq@mail.jlu.edu.cn

Acknowledgments

This work was supported by the Natural Science Foundation of China (Grant No.21003057) and the State Key Development Program for Basic Research of China (Grant No.2013CB834801) /the Jilin Provincial Natural Science Foundation (Grant No. 201215031)/Specialized Research Fund for the Doctoral Program of Higher Education (Grant No.20110061110018).

Notes and References

1. M. Irie, *Chem. Rev.*, 2000, **100**, 1685-1716.
2. T. Fukaminato, T. Kawai, S. Kobatake and M. Irie, *J. Phys. Chem. B*, 2003, **107**, 8372-8377.
3. A. Perrier, F. Maurel and D. Jacquemin, *Accounts. Chem. Res.*, 2012, **45**, 1173-1182.
4. T. Fukaminato, T. Doi, M. Tanaka and M. Irie, *J. Phys. Chem. C*, 2009, **113**, 11623-11627.
5. W. Tan, X. Li, J. Zhang and H. Tian, *Dyes. Pigments*, 2011, **89**, 260-265.
6. T. Fukaminato, T. Sasaki, T. Kawai, N. Tamai and M. Irie, *J. Am. Chem. Soc.*, 2004, **126**, 14843-14849.
7. K. Ouhenia-Ouadahi, R. Metivier, S. Maisonneuve, A. Jacquart, J. Xie, A. Leaustic, P. Yu and K. Nakatani, *Photochem. Photobiol.*, 2012, **11**, 1705-1714.
8. R. S. Sánchez, R. Gras-Charles, J. L. Bourdelande, G. Guirado and J. Hernando, *J. Phys. Chem. C*, 2012, **116**, 7164-7172.
9. T. Fukaminato, M. Tanaka, T. Doi, N. Tamaoki, T. Katayama, A. Mallick, Y. Ishibashi, H. Miyasaka and M. Irie, *Photochem. Photobiol.*, 2010, **9**, 181-187.
10. T. Fukaminato, T. Doi, N. Tamaoki, K. Okuno, Y. Ishibashi, H. Miyasaka and M. Irie, *J. Am. Chem. Soc.*, 2011, **133**, 4984-4990.
11. D. Guillaumont, T. Kobayashi, K. Kanda, H. Miyasaka, K. Uchida, S. Kobatake, K. Shibata, S. Nakamura and M. Irie, *J. Phys. Chem. A*, 2002, **106**, 7222-7227.
12. E. A. Perpète and D. Jacquemin, *J. Photochem. Photobiol. A*, 2007, **187**, 40-44.
13. F. Maurel, A. Perrier, E. A. Perpète and D. Jacquemin, *J. Photochem. Photobiol. A*, 2008, **199**, 211-223.
14. S. Aloise, M. Sliwa, Z. Pawlowska, J. Rehault, J. Dubois, O. Poizat, G. Buntinx, A. Perrier, F. Maurel, S. Yamaguchi and M. Takeshita, *J. Am. Chem. Soc.*, 2010, **132**, 7379-7390.
15. P. D. Patel and A. E. Masunov, *J. Phys. Chem. A*, 2009, **113**, 8409-8414.
16. D. Jacquemin and E. A. Perpete, *Chem. Phys. Lett.*, 2006, **429**, 147-152.
17. D. Jacquemin, C. Michaux, E. A. Perpete, F. Maurel and A. Perrier, *Chem. Phys. Lett.*, 2010, **488**, 193-197.
18. A. T. Bens, J. Ern, K. Kuldova, H. P. Trommsdorff and C. Kryschi, *J. Lumin.*, 2001, **94**, 51-54.
19. D. Jacquemin, A. Planchat, C. Adamo and B. Mennucci, *J. Chem. Theory. Comput.*, 2012, **8**, 2359-2372.
20. R. Send, M. Kühn and F. Furche, *J. Chem. Theory. Comput.*, 2011, **7**, 2376-2386.
21. T. Yanai, D. P. Tew and N. C. Handy, *Chem. Phys. Lett.*, 2004, **393**, 51-57.
22. C. Adamo and V. Barone, *J. Chem. Phys.*, 1999, **110**, 6158-6170.
23. A. D. Boese and J. M. L. Martin, *J. Chem. Phys.*, 2004, **121**, 3405-3416.
24. A. D. Becke, *J. Chem. Phys.*, 1993, **98**, 1372-1377.
25. J. P. Perdew, *Phys. Rev. B*, 1986, **33**, 8822-8824.
26. K. Okuno, Y. Shigeta, R. Kishi, H. Miyasaka and M. Nakano, *J. Photochem. Photobiol. A*, 2012, **235**, 29-34.
27. W. Li, J. Wang, J. Chen, F. Q. Bai and H. X. Zhang, *Spectrochimica acta. Part A, Molecular and biomolecular spectroscopy*, 2014, **118**, 1144-1151.
28. M. J. Frisch, G. W. Trucks, H. B. Schlegel, G. E. Scuseria, M. A. Robb, J. R. Cheeseman, V. G. Zakrzewski, J. A. Montgomery, Jr., R. E. Stratmann, J. C. Burant, S. Dapprich, J. M. Millam, A. D. Daniels, K. N. Kudin, M. C. Strain, O. Farkas, J. Tomasi, V. Barone, M. Cossi, R. Cammi, B. Mennucci, C. Pomelli, C. Adamo, S. Clifford, J. Ochterski, G. A. Petersson, P. Y. Ayala, Q. Cui, K. Morokuma, D. K. Malick, A. D. Rabuck, K. Raghavachari, J. B. Foresman, J. Cioslowski, J. V. Ortiz, B. B. Stefanov, G. Liu, A. Liashenko, P. Piskorz, I. Komaromi, R. Gomperts, R. L. Martin, D. J. Fox, T. Keith, M. A. Al-Laham, C. Y. Peng, A. Nanayakkara, C. Gonzalez, M. Challacombe, P. M. W. Gill, B. G. Johnson, W. Chen, M. W. Wong, J. L. Andres, M. Head-Gordon, E. S. Replogle and J. A. Pople, *Gaussian 09* (2009) Gaussian, Inc, Wallingford CT.
29. Y. C. Jeong, S. I. Yang, K. H. Ahn and E. Kim, *Chem. Commun.*, 2005, 2503-2505.
30. T. Fukaminato, M. Tanaka, L. Kuroki and M. Irie, *Chem. Commun.*, 2008, 3924-3926.
31. M. T. Indelli, S. Carli, M. Ghirotti, C. Chiorboli, M. Ravaglia, M. Garavelli and F. Scandola, *J. Am. Chem. Soc.*, 2008, **130**, 7286-7299.
32. P. R. Hania, A. Pugzlys, L. N. Lucas, J. J. D. de Jong, B. L. Feringa, J. H. van Esch, H. T. Jonkman and K. Duppen, *J. Phys. Chem. A*, 2005, **109**, 9437-9442.
33. M. Boggio-Pasqua, M. Ravaglia, M. J. Bearpark, M. Garavelli and M. A. Robb, *J. Phys. Chem. A*, 2003, **107**, 11139-11152.
34. A. Staykov, J. Areephong, W. R. Browne, B. Feringa and K. Yoshizawa, *ACS NANO*, 2011, **5**, 1165-1178.
35. Y. Asano, A. Murakami, T. Kobayashi, A. Goldberg, D.

Guillaumont, S. Yabushita, M. Irie and S. Nakamura, *J. Am. Chem. Soc.*, 2004, **126**, 12112-12120.
36. P. R. Hania, R. Telesca, L. N. Lucas, A. Pugzlys, J. van Esch, B. L. Feringa, J. G. Snijders and K. Duppen, *J. Phys. Chem. A*, 2002, **106**, 8498-8507.
37. A. Perrier, F. Maurel and D. Jacquemin, *J. Phys. Chem. C*, 2011, **115**, 9193-9203.
38. A. Perrier, F. Maurel and D. Jacquemin, *Chem. Phys. Lett.*, 2011, **509**, 129-133.
39. D. Jacquemin, E. A. Perpete, F. Maurel and A. Perrier, *J. Phys. Chem. C*, 2010, **114**, 9489-9497.
40. M. Cipolloni, A. Heynderickx, F. Maurel, A. Perrier, D. Jacquemin, O. Siri, F. Ortica and G. Favaro, *J. Phys. Chem. C*, 2011, **115**, 23096-23106.
41. J. Areephong, W. R. Browne and B. L. Feringa, *Org. Biomol. Chem.*, 2007, **5**, 1170-1174.